Dynamic Modeling of Semi-Active Suspension with Air Spring and Tire-Road Interaction

Carlos Cesar Augusto Itacaramby, Marcus Vinicius Girão de Morais

Mechanical Engineering Department, University of Brasilia
Campus Darcy Riberio,s/n, 71.910-000, Brasilia,DF, BRAZIL
cc.itacaramby@gmail.com; mvmorais@unb.br

Abstract. Excessive vibrations transmitted to the driver in a vehicle can negatively impact human health. Consequently, in recent years, research has focused on developing suspension models that improve comfort and drivability. The present work aims to model the semi-active suspension of a ¼ vehicle using an air spring. The semi-active skyhook control strategy was explored for comparison with passive systems. The study of the air suspension was evaluated from the perspective of comfort and drivability, using metrics such as root mean square (RMS) and analyses of the response signal behavior. The quarter car models were simulated in the MATLAB/Simulink environment and showed that models with air springs provide more comfort and drivability for the vehicle.

Keywords: Air spring with a damper, vehicle dynamics, semi-active skyhook control

1 Introduction

Excessive vibration that reaches the driver's body in a vehicle can be harmful to human health. Therefore, over the past few years, research has been conducted to propose suspension models that enhance vehicle comfort and drivability. Depending on the control method, a suspension model, according to Mutar and Abdalla [1], can be classified as passive, semi-active, or active. Crivellaro [2] characterizes the passive system as one that does not use an external energy source, making this type of model simple and reliable. Corrêa [3] describes that active systems are quite effective in controlling the vehicle body movements but generally do not have the same efficiency in body isolation when excited at high frequencies. Yao [4] describes that the semi-active system combines the advantages of active and passive suspensions, as it is safe and does not require high-power actuators or large power supplies to change stiffness/damping parameters instantaneously.

According to Barethiye [5], the suspension system consists of a shock absorber and a spring installed in parallel, where the shock absorber dissipates the vibration energy of the suspension when the vehicle passes over a road excitation source. Xie [6] researched that the spring absorbs the road excitation by compressing and releases this stored energy to the vehicle body by gradually expanding. Among the various types of vehicle springs, air springs are widely used in heavy trucks and train carriages because of their behavior in using a compressible fluid in their operation. Following is a brief review of air springs. Quaglia, Giuseppe, and Sorli [7] present a dimensionless model of a pneumatic suspension, focusing on the correct selection of parameters to avoid excessive amplification near resonance. Chang and Lu [8] propose a more accurate dynamic model for pneumatic springs, validating it experimentally and integrating it into a MATLAB/Simulink simulation model. Lee [9] develops a general analytical model for pneumatic springs, considering stiffness nonlinearities and hysteresis effects to improve the design of vehicles with these suspensions. Gavriloski, Viktor, et al [10] present a dynamic model of a pneumatic spring with frequency-dependent characteristics, exploring how changes in damping and stiffness coefficients can improve comfort and drivability. Franz [11] develops a control model for an active pneumatic suspension system, aiming to balance comfort and control. MATLAB/Simulink simulations demonstrate the system's effectiveness in different driving scenarios compared to a passive system. Mohammed, Mortda, and Alktranee [12] investigate three strategies for suspension system behavior: replacing coil springs with pneumatic springs, applying an on/off logic control to the air mass of the pneumatic spring, and using a magneto-rheological (MR) damper for variable damping. The results show that pneumatic springs and semi-active strategies improve suspension quality. Zhang, Bangji, et al. [13] experimentally research a semi-active air spring model. Numerical simulations validate the control strategy's effectiveness, showing significant improvements in suspension comfort. Melo [14] proposes a semi-active skyhook suspension model, which adjusts damping based on terrain frequency, comparing it with existing passive and semi-active models and active systems.

The present work aims to model the semi-active suspension of a ¼ vehicle using an air spring. The semi-active skyhook control strategy was explored for comparison with passive systems. The study of the air suspension was evaluated from the perspective of comfort and drivability, using metrics such as root mean square (RMS) and analyses of the response signal behavior. The quarter-car models were simulated in the MATLAB/Simulink environment and showed that models with air springs provide more comfort and drivability for the vehicle.

Section 2 of this article includes the governing equations and mathematical models of the vehicle, Section 3 covers the skyhook strategy and control system, Section 4 describes the road inputs excitation, Section 5 the performance metrics, Section 6 explains the methodology and computational model implementation, the results are presented in Section 7, and finally, the conclusion is in Section 8.

2 Quarter vehicle with air spring suspension

In this study, a quarter vehicle model is considered for the analyses. The passive system, it consists of a two-degree-of-freedom model with a sprung mass (vehicle mass), an unsprung mass (tire assembly), a damper, and a spring. This structure can be observed in Figure 1.

The equations (1)-(3) related to the suspension dynamics of the quarter vehicle model are presented below:

$$m_s\ddot{x}_s = -F_{spring} - F_{damper}, \tag{1}$$

$$m_u\ddot{x}_u = F_{spring} + F_{damper} - F_{tire}, \tag{2}$$

where m_s is the sprung mass, m_u is the unsprung mass, x_s is the displacement of the sprung mass, x_u is the displacement of the unsprung mass, F_{damper} is the damper force, F_{tire} is the dynamic tire force, and F_{spring} is the spring force. In the case of a passive system, the forces can be described as:

$$F_{spring} = k_s(x_s - x_u)\ , \qquad F_{damper} = c_s(\dot{x}_s - \dot{x}_u)\ , \qquad F_{tire} = k_u(x_u - z), \tag{3}$$

2.1 Air spring model

The air suspension system can be divided into four parts: an air bag, an air reservoir, a connection tube, and a control valve (on/off). The schematic model of the passive system can be seen in Figure 1a, on the left. The air spring system is shown in Figure 1b, on the right.

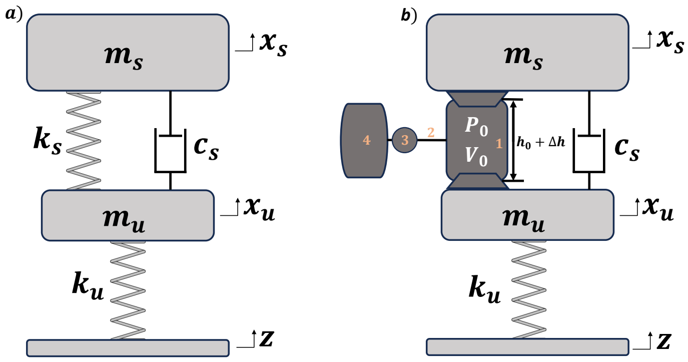

Figure 1. Schematic description of a quarter-vehicle system representation of (a) linear quarter of vehicle and (b) air spring quarter of vehicle. The index 1 in orange represents the air bag, 2 the connecting pipe, 3 the control valve (on/off), and 4 the reservoir.

Essentially, air springs are chambers of thin, flexible, rubberized fabric with walls containing pressurized air. Zhang, Bangji, et al. [13] made the assumptions that the gas inside the air bag is considered an ideal gas, the process of changing the gas state in the pneumatic spring is considered a quasi-static process, and the pneumatic spring is neither fully inflated nor deflated but has an initial pressure P_0 and an initial volume V_0. Thus, the force exerted by such springs can be expressed by the relation:

$$F_{spring} = F_{air} = (P - P_a)A_e, \tag{4}$$

where P is the absolute pressure in the air spring at that instant, P_a is the atmospheric pressure, and A_e is the effective area.

According to Quaglia, Giuseppe, and Sorli [7], the effective area is an imaginary, non-constant area on which the internal pressure of the spring is presumed to act. Since this area does not correspond to a geometrically defined value, it is evaluated through constant internal pressure tests where the force F is measured while varying the height h. Based on the work of Zhang, Bangji, et al. [13], the following relation for the effective area can be used:

$$A_e = -531\Delta h^5 - 4.68\Delta h^4 + 10.6\Delta h^3 - 0.601\Delta h^2 + 0.00261\Delta h + 0.0451, \tag{5}$$

where Δh is the variable deformation of the air spring.

Considering now that the air spring is actuated quickly enough for all the operational heat to be conserved, an adiabatic process occurs and can be expressed as:

$$PV^n = P_0 V_0^n = const, \tag{6}$$

where V is the volume of the air spring at that instant, and n is the ratio of the specific heats of the gas at constant pressure and constant volume. Presthus [15] analyzed that during normal operation, the pneumatic process is not fast enough to be adiabatic nor slow enough to be isothermal, classifying it as polytropic.

Thus, V can be described by the equation:

$$V = (h_0 - \Delta h)A_e, \tag{7}$$

where h_0 is the initial height of the air spring.

Combining eq. (4) with eq. (7), the force of the air spring at that instantat can be described as:

$$F_{air} = \left(\frac{P_0 V_0^n}{[A_e(h_0 - \Delta h)]^n} - P_a\right)A_e. \tag{8}$$

Thus, the stiffness of the spring can be obtained by differentiating the force with respect to the deformation.

$$k = \frac{dF_{air}}{d(\Delta h)} = P_0 V_0^n \frac{kA_e^2 - (k-1)(h_0 - \Delta h)A_e}{[A_e(h_0 - \Delta h)]^{n+1}} \frac{dA_e}{d(\Delta h)} - P_a \frac{dA_e}{d(\Delta h)}. \tag{9}$$

3 Semi-active control via skyhook

The skyhook approach primarily focuses on the sprung mass. As the fictitious damping coefficient c_{sky} increases, the isolation of the mass from road excitation improves. However, this results in a significant increase in the vertical displacement of the unsprung mass. The equations that describe the suspension are given by:

$$m_s \ddot{x}_s = -k_s(x_s - x_u) - c_{sky}\dot{x}_s, \tag{10}$$

$$m_u \ddot{x}_u = k_s(x_s - x_u) - k_u(x_u - z). \tag{11}$$

Thus, it is possible to isolate the coefficient c_s [14]. In this case, the damping is a function that depends on the displacement of both the sprung and unsprung masses, obtained from the skyhook approach.

$$c_s = \frac{2\zeta_{sky}\dot{x}_s\sqrt{k_s m_s}}{\dot{x}_u - \dot{x}_s}. \tag{12}$$

The logic criterion for the control system depends on the velocity values of the sprung and unsprung masses such that if $\dot{x}_s(\dot{x}_s - \dot{x}_u) > 0$, the valve is on, and if $\dot{x}_s(\dot{x}_s - \dot{x}_u) \leq 0$, the valve is off.

4 Road inputs excitation

The quarter vehicle model is simulated under different types of road excitation. The different profiles and their parameters are described below.

The unit step input is a common excitation in control engineering, as see in Figure 2. The characteristics observable in this transient response include the delay time (t_d), rise time (t_r), peak time (t_p), maximum peak value (X_{over}), and settling time (t_s) [16].

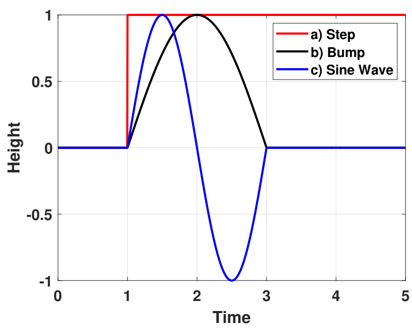

Figure 2. Road excitations in the time domain were (a) is step unit (red line) (b) is bump wave (blue line) (c) is sine wave (black line).

Others two excitation inputs are bump wave input and harmonic sine wave. The difference between boths are that bump wave is an excitation input with a quarter of harmonic sine wave length, as described in Figure 2.

Another road excitation used is the SAE road profile. Mahmood, Nassar, and Mohammad [17] studied that suspension behavior can be investigated using a random road profile generated from white noise filtering. The equation below shows the mathematical model of road roughness, where G_q represents the road roughness coefficient, defined for typical values of road classes from A to F [18], n_0 is a spatial frequency and is equal to $0.1\,\mathrm{m}^{-1}$, f_0 is a minimum cutoff frequency equal to 0.0628 Hz, $v(t)$ is the vehicle speed, and $w(t)$ is the white noise signal:

$$\dot{z}(t) + 2\pi f_0 z(t) = 2\pi n_0 \sqrt{G_q(n_0) v(t) w(t)}. \tag{13}$$

5 Performance criterion

The comfort quality criterion can be represented by the root mean square (RMS) value of the acceleration and displacement of the sprung mass, which can be calculated as follows:

$$RMS_{acc} = \sqrt{\frac{1}{T}\int_0^T \ddot{x}_s^2\, dt}, \tag{14}$$

$$RMS_{dis} = \sqrt{\frac{1}{T}\int_0^T x_s^2\, dt}. \tag{15}$$

The dynamic tire force indicates the road grip and vehicle safety on the road. The RMS value in the time domain can be calculated as follows:

$$RMS_{dtf} = k_u \sqrt{\frac{1}{T}\int_0^T (x_u - z)^2\, dt}. \tag{16}$$

6 Methodology and computational implementation

To verify the performance of the suspension systems, four different types of models were simulated: a passive suspension system, a passive suspension system with skyhook, a semi-active suspension system with an air spring, and a semi-active suspension system with an air spring and skyhook.

The SAE road excitation described in section 4 is simulated using a Simulink program to perform the necessary interactions. The mathematical model follows the formulations in sections 2.1 and 3, and is simulated using a MATLAB code that employs an adapted fourth-order Runge-Kutta method. The adaptation involves creating a loop that, at each interaction, calculates the coefficient c_s defined in eq. (12) and checks the velocity condition from section 3 to determine whether the valve should be on or off. Subsequently, the Runge-Kutta coefficients are computed to output the displacement, velocity, and acceleration values for the sprung and unsprung masses, as done in Melo's study [14].

7 Results and discussion

The performance of the suspension models was analyzed in this study through the comparison of characteristics observed with step excitation, and the comfort and handling were studied by comparing the RMS of acceleration, displacement, and tire force. The simulation was carried out using the skyhook control strategy for the quarter vehicle model, with various configurations for the suspension models. Comfort during driving improves with lower RMS values of the sprung mass acceleration. The dynamic tire force reflects the vehicle's grip on the road; higher dynamic forces indicate reduced adhesion and safety due to insufficient contact between the tire and the road surface. However, it is preferable to have the highest possible RMS for potential energy recovery.

The suspension parameters adopted for the simulation were 800 kg for m_s, 50 kg for m_u, 23390 N/m for k_s in the passive and passive skyhook systems, 100000 N/m for k_u, 1200 Ns/m for c_s, 0.7 MPa for P_0, 0.1 MPa for P_{at}, 0.095 m^3 for V_0, 1.381 for n, and 0.252 m for h_0.

The performance characteristics, described in Section 4, are as follows: The delay time (t_d) for the passive spring was 20.0 s, 21.3 s for the passive skyhook, 28.7 s for the air spring, and 28.9 s for the air spring with skyhook. For the rise time (t_r), the passive spring system recorded 31.8 s, the skyhook system 31.0 s, the air spring 39.5 s, and the air spring with skyhook 39.4 s. The peak time (t_p) was 61.5 s for the passive spring, 61.7 s for the skyhook system, 66.5 s for the air spring, and 67.2 s for the air spring with skyhook. Finally, the overshoot (X_{over}) was 49.9% for the passive spring, 49.1% for the skyhook system, 40.0% for the air spring, and 39.1% for the air spring with skyhook.

The parameters of the suspension systems reveal that for comfort applications, a quick and well-damped response is desirable. Comparing the systems, it is observed that skyhook systems perform similarly to normal systems, with minimal differences compared to the passive system and the air spring system. In particular, air spring systems exhibit larger delay, rise, and peak times, which may indicate greater comfort compared to the passive system. Additionally, pneumatic models show lower overshoot, a smaller peak in displacement signal, contributing to increased comfort.

The comparison of the sprung mass displacement signal for the four types of systems under different road excitations can be observed in figures 3a, 4a and 5a. In all cases, there is a reduction in the sprung mass displacement signal compared to the passive system. Additionally, the behavior of the sprung mass acceleration and tire dynamic force was simulated for each type of excitation. For sinusoidal excitations, the results are shown in comparison form in figures 3b and 4b. For random road excitation, the results for tire dynamic load and acceleration are presented in figures 5b and c, while figure 5d shows a comparison of the results in RMS form.

In all cases, the air spring system offered greater comfort, safety, and drivability. For bump excitation, air spring systems significantly reduced sprung mass displacement, while skyhook systems excelled in acceleration and tire force. For sinusoidal excitation, the air spring system had 9.2% lower RMS displacement and 12.4% lower RMS acceleration compared to the skyhook model. Conversely, for random road profiles, the pneumatic spring showed the best performance in acceleration and tire force, with both air spring alone and air spring with skyhook outperforming the passive skyhook system.

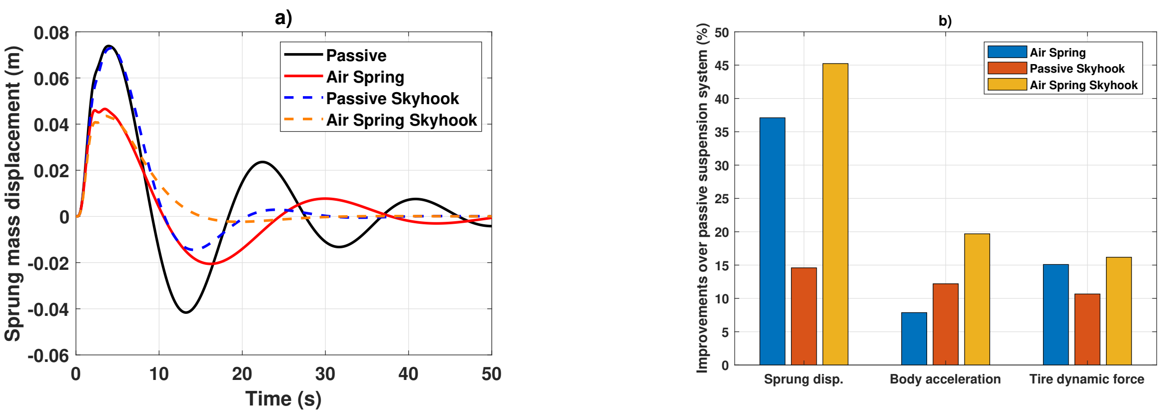

Figure 3. Dynamic results for bump excitation for passive and air-spring quarter vehicle suspension with/without skyhook semi-active control. Figure (a) shows time history of sprung mass displacement, while (b) shows comparison of improvement per report to passive quarter vehicle suspension as function of performance criterium eq. (14)-(15).

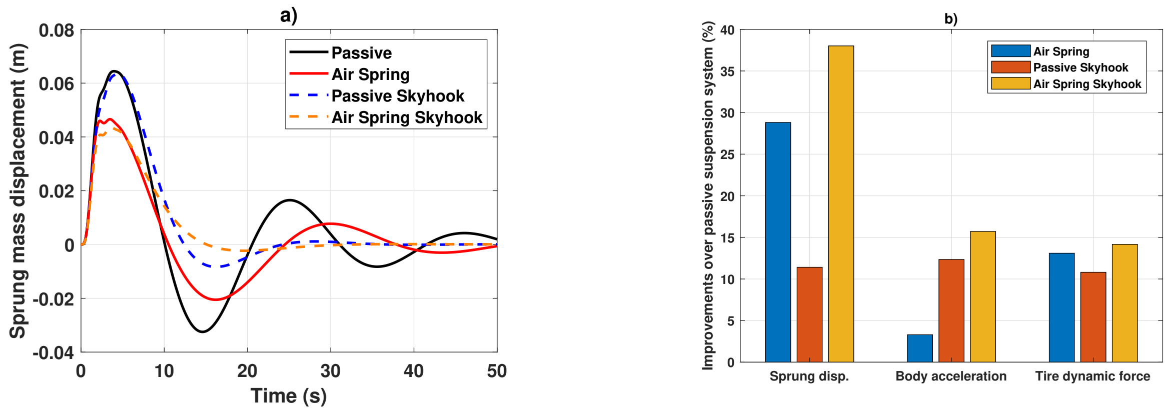

Figure 4. Dynamic results for sine wave excitation for passive and air-spring quarter-vehicle suspension with/without skyhook control. Figure (a) shows the sprung mass displacement, while (b) compares improvements relative to passive suspension based on performance criteria eq. (14)-(15).

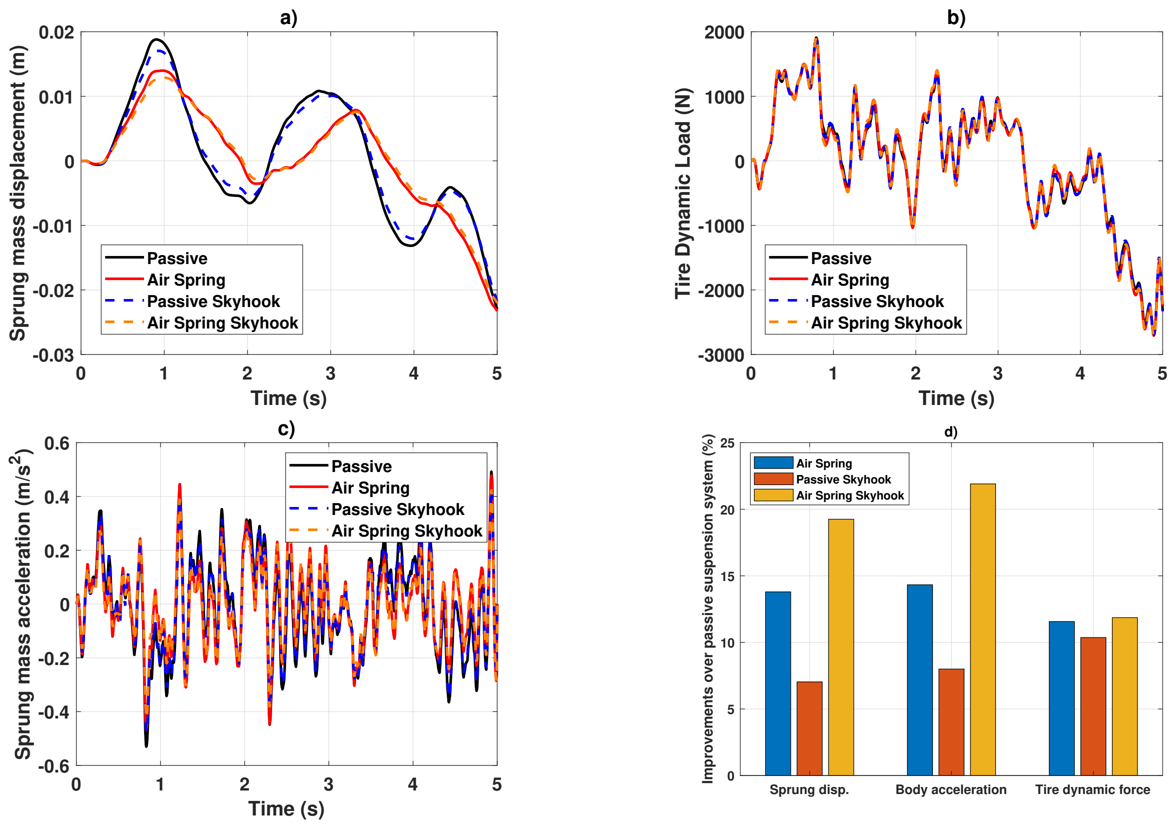

Figure 5. Dynamic results for random road excitation (Class C, 20 m/s) for passive and air-spring quarter-vehicle suspension with/without skyhook control. Figure (a) shows the sprung mass displacement, (b) the tire load signal, (c) the suspended mass accelerations, and (d) a comparison of improvements relative to passive suspension based on performance criteria eq. (14)-(16).

8 Conclusion

A pneumatic spring was simulated using a quarter-vehicle model to investigate its dynamic characteristics with four different suspension systems. Results were compared using RMS values for various suspension styles and signals. Responses were evaluated for step, harmonic, and random road inputs. For random road excitations, passive suspension with skyhook, pneumatic spring, and pneumatic spring with skyhook reduced maximum suspended mass acceleration by 8.0%, 14.3%, and 21.9%, respectively, compared to the passive system. Future studies may include a detailed analysis of lateral dynamics using air springs to examine other suspension parameters such as roll sensitivity, roll center, and lateral rollover limit, in order to assess the vehicle's behavior in curves.

Acknowledgements. The authors would like to acknowledge the support of the University of Brasília, CNPq, and FAPDF for providing the necessary support and equipment to conduct the research.

Authorship statement. The authors hereby confirm that they are the sole liable persons responsible for the authorship of this work, and that all material that has been herein included as part of the present paper is either the property (and authorship) of the authors.

References

[1] W. H. Al-Mutar and T. Y. Abdalla. Quarter car active suspension system control using fuzzy controller tuned by pso. *International journal of computer applications*, vol. 127, n. 2, pp. 38–43, 2015.
[2] C. Crivellaro. *Controle robusto de suspensão semi-ativa para caminhonetes utilizando amortecedores magneto-reológicos.* PhD thesis, Universidade de São Paulo, 2008.
[3] J. L. Corrêa. Comportamento dinâmico de um veículo implementado com suspensões ativas. Master's thesis, Universidade Federal do Rio Grande do Sul, 2011.
[4] G. Yao, F. Yap, G. Chen, W. Li, and S. Yeo. Mr damper and its application for semi-active control of vehicle suspension system. *Mechatronics*, vol. 12, n. 7, pp. 963–973, 2002.
[5] V. Barethiye, G. Pohit, and A. Mitra. Analysis of a quarter car suspension system based on nonlinear shock absorber damping models. *International Journal of Automotive and Mechanical Engineering*, vol. 14, n. 3, pp. 4401–4418, 2017.
[6] X. Xie and Q. Wang. Energy harvesting from a vehicle suspension system. *Energy*, vol. 86, pp. 385–392, 2015.
[7] G. Quaglia and M. Sorli. Air suspension dimensionless analysis and design procedure. *Vehicle System Dynamics*, vol. 35, n. 6, pp. 443–475, 2001.
[8] F. Chang and Z. Lu. Dynamic model of an air spring and integration into a vehicle dynamics model. *Proceedings of the Institution of Mechanical Engineers, Part D: Journal of Automobile Engineering*, vol. 222, n. 10, pp. 1813–1825, 2008.
[9] S. Lee. Development and analysis of an air spring model. *International Journal of Automotive Technology*, vol. 11, pp. 471–479, 2010.
[10] V. Gavriloski, J. Jovanova, G. Tasevski, and M. Ðidrov. Development of a new air spring dynamic model. *FME Transactions*, vol. 42, n. 4, pp. 305–310, 2014.
[11] D. Franz. *Simulink control model of an active pneumatic suspension system for passenger cars*. PhD thesis, Politecnico di Torino, 2019.
[12] M. Mohammed and M. H. Alktranee. Parametric analysis of vehicle suspension based on air spring and mr damper with semi-active control. In *Journal of physics: conference series*, volume 1773, pp. 012022. IOP Publishing, 2021.
[13] B. Zhang, M. Liu, K. Wang, B. Tan, Y. Deng, A. Qin, and J. Liu. Takagi–sugeno fuzzy model-based control for semi-active cab suspension equipped with an electromagnetic damper and an air spring. *Machines*, vol. 11, n. 2, pp. 226, 2023.
[14] M. A. Melo. Análise comparativa de estratégias para suspensão semiativa em um modelo de 1/4 de veículo. Universidade de Brasília, 2017.
[15] M. Presthus. Derivation of air spring model parameters for train simulation. Master's thesis, Luleå University of Technology, 2002.
[16] K. Ogata, H. C. d. Souza, and E. A. Tannuri. *Engenharia de controle moderno*. Pearson Education do Brasil, 1998.
[17] M. S. Mahmood, A. A. Nassar, and H. M. Mohammad. Analysis and study indicators for quarter car model with two air suspension system. *Basrah Journal for Engineering Sciences*, vol. 22, pp. 16–22, 2022.
[18] T. C. ISO/TC, M. Vibration, S. S. S. Measurement, of E. Mechanical Vibration, and as Applied to S. Machines. *Mechanical Vibration–Road Surface Profiles–Reporting of Measured Data*, volume 8608. International Organization for Standardization, 1995.